Mechanistic Role of an NS4A Peptide Cofactor with the Truncated NS3 Protease of Hepatitis C Virus: Elucidation of the NS4A Stimulatory Effect *via* Kinetic Analysis and Inhibitor Mapping

James A. Landro,* Scott A. Raybuck, Yu Ping C. Luong, Ethan T. O'Malley, Scott L. Harbeson, Kurt A. Morgenstern, Govinda Rao, and David J. Livingston

Vertex Pharmaceuticals Incorporated, 130 Waverly Street, Cambridge, Massachusetts 02139-4242

Received December 12, 1996; Revised Manuscript Received May 12, 1997[⊗]

ABSTRACT: Infection by hepatitis C viruses (HCVs) is a serious medical problem with no broadly effective treatment available for the progression of chronic hepatitis. The catalytic activity of a viral serine protease located in the N-terminal one-third of nonstructural protein 3 (NS3) is required for polyprotein processing at four site-specific junctions. The three-dimensional crystal structure of the NS3−NS4A co-complex [Kim, J. L., Morgenstern, K. A., Lin, C., Fox, T., Dwyer, M. D., Landro, J. A., Chambers, S. P., Markland, W., Lepre, C. A., O'Malley, E. T., Harbeson, S. L., Rice, C. M., Murcko, M. A., Caron, P. R., & Thomson, J. A. (1996) *Cell 87,* 343−355] delineates a small hydrophobic region within the 54-residue NS4A protein that intercalates with and makes extensive contacts to the core of the protease. The current investigation addresses the mechanism of NS3 protease catalytic activation by NS4A utilizing a small synthetic NS4A peptide (residues 1678−1691 of the virus polyprotein sequence) and the recombinantly expressed protease domain of NS3. The addition of NS4A dramatically increased NS3 k_{cat} and k_{cat}/K_m catalytic parameters when measured against small peptide substrates representing the different site-specific junctions of the polyprotein. The catalytic effect of natural and non-natural amino acid substitutions at the P_1 position in a 5A/5B peptide substrate was investigated. NS3−NS4A demonstrated a marked catalytic preference for the cysteine residue commonly found in authentic substrates. The pH dependence of the NS3 hydrolysis reaction is not affected by the presence of NS4A. This result suggests that NS4A does not change the pK_a values of the active site residues of NS3 protease. A steady state kinetic analysis was performed and indicated that the binding of NS4A and the peptide substrate occurs in an ordered fashion during the catalytic cycle, with NS4A binding first. Two distinct kinetic classes of peptidyl inhibitors based upon the 5A/5B cleavage site were identified. An NS4A-independent class is devoid of prime residues. A second class of inhibitors is NS4A-dependent and contains a natural or non-natural cyclic amino acid substituted for the commonly found P_1' residue serine. These inhibitors display an up to 80-fold increase in affinity for NS3 protease in the presence of NS4A. Sequential truncation of prime and P residues from this inhibitor class demonstrated the fact that the P_4' and P_1' residues are crucial for potent inhibition. The selectivity of this NS4A effect is interpreted using a model of the 5A/5B decapeptide substrate bound to the active site of the NS3−NS4A structure.

The hepatitis C virus (HCV)[1] genus of the flavivirus family is responsible for widespread and potentially fatal liver diseases (Kuo et al., 1989; Houghton et al., 1991). Current estimates indicate that >1% of the human population is infected by the positive-strand RNA HCV. Protective vaccines are not available, and α-interferon, the only approved therapy, is effective in fewer than 25% of the cases. Alternate therapeutic approaches aimed toward controlling viral replication need to be investigated (Houghton, 1996), and this has stimulated efforts to characterize HCV proteins as targets for inhibitor design.

Hepatitis C viruses contain a positive-sense RNA genome of 9.4 kilobases with a single open reading frame encoding a polyprotein of 3010−3033 amino acids (Kato et al., 1990; Choo et al., 1991; Takamizawa et al., 1991; Grakoui et al., 1993c). The translated HCV polyprotein is proteolytically processed by a combination of host- and virus-encoded enzymes into nine distinct polypeptides: 5′-C-E1-E2-NS2-NS3-NS4A-NS4B-NS5A-NS5B-3′. Structural proteins C (nucleocapsid), E1, and E2 are excised from the HCV polyprotein by a host-encoded endoplasmic reticulum signal peptidase (Hijikata et al., 1991; Lin et al., 1994a; Mizushima et al., 1994). The generation of mature nonstructural viral proteins is catalyzed by proteases encoded by the virus genome (Figure 1). Hydrolysis at the NS2/NS3 junction is

* To whom correspondence should be addressed. Telephone: 617-577-6000. Fax: 617-577-6437.

[⊗] Abstract published in *Advance ACS Abstracts,* July 15, 1997.

[1] Abbreviations: α-Abu, α-aminobutyric acid; DMSO, dimethyl sulfoxide; DTT, dithiothreitol; Fmoc, fluorenylmethoxycarbonyl; HBTU, *O*-benzotriazol-1-yl-*N*,*N*,*N*′,*N*′,-tetramethyluronium hexaflurophosphate; HOBt, hydroxybenztriazole; HCV, hepatitis C virus; HEPES, *N*-(2-hydroxyethyl)piperazine-*N*′-2-ethanesulfonic acid; HPLC, high-performance pressure liquid chromatography; KK4A, amino acids 1678−1691 of the HCV polyprotein sequence encompassing a hydrophobic region of NS4A and containing two additional non-HCV N-terminal lysine residues; MALDI, matrix-assisted laser desorption ionization; MES, 2-(*N*-morpholino)ethanesulfonic acid; 2Nal, 2-naphthylalanine; Nle, norleucine; NS, nonstructural; Phg, phenylglycine; Pip, pipecolinic acid; PMSF, phenylmethanesulfonyl fluoride; pNA, *p*-nitroanilide; TFA, trifluoracetic acid; Tic, tetrahydroisoquinoline-3-carboxylic acid; tNS3, protease domain of NS3 generated by truncation of residues from the C terminus of the full length protein.

S0006-2960(96)03054-1 CCC: $14.00

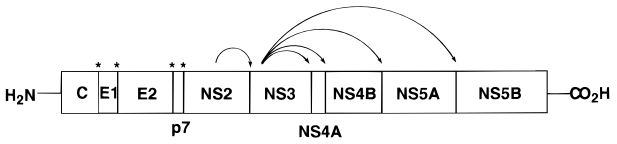

FIGURE 1: HCV polyprotein processing. The locations of structural and nonstructural HCV proteins are indicated on the 3011-amino acid polyprotein. Asterisks mark the locations of cleavages catalyzed by host-encoded proteases. Cleavage between the NS2/NS3 junction is mediated by the NS2/NS3 protease. The NS3 protease catalyzes hydrolysis between the NS3/NS4A, NS4A/NS4B, NS4B/NS5A, and NS5A/NS5B junctions.

catalyzed by an incompletely characterized Zn^{2+}-dependent protease comprising NS2 and the N-terminal domain of NS3 (Grakoui et al., 1993b; Hijikata et al., 1993). Processing at the NS3/NS4A, NS4A/NS4B, NS4B/NS5A, and NS5A/NS5B sites is catalyzed by the NS3 protein (Bartenschlager et al., 1993; Eckart et al., 1993; Grakoui et al., 1993a; Hijikata et al., 1993; Tomei et al., 1993; Manabe et al., 1994). Characterization of NS3-catalyzed proteolysis activity indicates that processing at the NS3/NS4A junction is an intramolecular event (occurring in *cis*), while intermolecular processing (in *trans*) is permitted at other junctions. Sequence analysis of individual cleavage sites indicates that the intermolecular consensus sequence site[2] D/E-X-X-X-X-C*-A/S differs from the intramolecular cleavage site by substitution of Thr for Cys at the P_1 position (Grakoui et al., 1993a; Pizzi et al., 1994).

A body of experimental evidence demonstrated that the 70 kDa NS3 protein is composed of two domains: a protease domain encompassing the amino-terminal one-third of the protein and an ATP-dependent RNA helicase domain encompassing the C-terminal two-thirds (Miller & Purcell, 1990; Bartenschlager et al., 1993; Eckart et al., 1993; Grakoui et al., 1993a; Tomei et al., 1993). The X-ray crystal structures recently published by Kim et al. (1996) and by Love et al. (1996) of the NS3 protease domain provide the first structural analysis of a protease from the flavivirus family. The protease has a chymotrypsin-like fold, an active site catalytic triad, and a tetrahedrally coordinated metal ion distal to the active site. In addition, the apposition of the catalytic triad residues (Asp1107, His1083, and Ser1185) and the positions of the backbone amides of Gly1163 and Ser1165 which form the oxyanion hole are similar to the active site topography of other chymotrypsin-like enzymes (Kim et al., 1996; Love et al., 1996). These two published structures differ in one critical feature. The structure determined by Love et al. (1996) is of NS3 protease alone. Kim et al. (1996), however, determined the structure of the NS3−NS4A co-complex. In this co-complex, a 19-residue NS4A peptide encompassing a hydrophobic region of the protein (Gly21−Lys34) binds between strands A_0 and A_1 of the N-terminal domain of NS3 protease and contributes one of eight total β strands to the core. Extensive hydrogen bonding between main chain carbonyl and amide residues of Val23−Leu31 of NS4A and the N-terminal region of NS3 or strand A_1 is observed, with a total of 2400 Å^2 of surface area buried by the interaction between them (Kim et al., 1996).

[2] The asterisk indicates the site of hydrolysis and is referenced as the P_1 residue according to the nomenclature of Schechter and Berger (Schechter, 1967).

A number of biochemical observations corroborate the proximity of NS3−NS4A observed in the co-complex structure and suggest NS3−NS4A is the biologically relevant and catalytically active species in solution. Transfection experiments have shown that the 54-residue NS4A protein accelerates the basal NS3-catalyzed rate of hydrolysis at the NS4A/NS4B and the NS5A/NS5B junctions and that it is an obligate cofactor for cleavage at the NS4B/NS5A junction (Failla et al., 1994; Lin et al., 1994b). Immunoprecipitation and mutational analysis studies suggest stable and extensive interactions between the N-terminal protease domain of NS3 and the central hydrophobic region of NS4A encompassing residues Gly21−Lys34 (Failla et al., 1995; Lin et al., 1995; Satoh et al., 1995). Using small peptide substrates, the catalytic activity of the NS3 protease domain has been shown to be stimulated up to 100-fold in the presence of an NS4A peptide (Failla et al., 1994; Shimizu et al., 1996; Steinkuhler et al., 1996b). Although these studies demonstrate the *in vivo* catalytic utility of NS4A and quantitate the *in vitro* stimulatory effect, they provide little insight into the kinetic mechanism utilized by NS4A in the activation of NS3.

The present study defines the kinetic role of an NS4A peptide in the catalytic activation of the NS3 protease domain and probes the specificity of the NS3−NS4A complex toward amino acid substitutions at the P_1 and P_1' positions of peptide substrates. The data suggest NS4A modulates NS3 protease activity by alteration of S′ subsites and are consistent with interactions observed within the NS3−NS4A co-complex structure.

EXPERIMENTAL PROCEDURES

General. The expression and purification of the N-terminal 181 amino acids of the NS3 protease domain (tNS3) from hepatitis C virus strain H in *Escherichia coli* was performed as described previously (Kim et al., 1996).

Peptides and Assays. Peptides EDVVαAbuCSMSY (αAbu designates α-aminobutyric acid), DEMEECSQHLPYI, ECTTPCSGSWLRD, and EDVVαAbuC-*p*-nitroanilide were purchased from AnaSpec Inc. (San Jose, CA).

Other peptides were prepared by the solid phase peptide synthesis method (Advanced ChemTech 396 MPS or Applied Biosystems 433A apparatus) beginning with the appropriate N^{α}-Fmoc aminoacyl Wang resin. N^{α}-Fmoc-protected amino acids were added sequentially using HBTU with HOBt as coupling agents in *N*-methylpyrrolidinone. Cleavage from the resin and global deprotection were accomplished with 95% trifluoroacetic acid and 5% water at room temperature for 1.5 h [15 mL/(g of resin)]. The peptides were purified by preparative high-performance liquid chromatography (HPLC) on a Waters Delta Pak C18, 15 μm, 300 Å column (30 mm × 300 mm), eluting with a linear gradient of acetonitrile in 0.1% aqueous trifluoroacetic acid over 35 min at a flow rate of 22 mL/min. Lyophilization yielded the peptides, which were characterized for purity by analytical HPLC (Hewlett-Packard 1050 Series instrument) on a Waters Delta Pak C18, 5 μm, 300 Å column (3.9 mm × 150 mm). All peptides yielded the correct $(M + H)^+$ and $(M + Na)^+$ molecular ions by matrix-assisted laser desorption mass spectrometry (Kratos MALDI I). Peptide content was determined by quantitative nitrogen microanalysis (Galbraith Laboratories Inc., Knoxville, TN) or quantitative N-terminal amino acid analysis, and the appropriate values were used

in preparing stock peptide solutions. pK_a determinations were determined by Robertson Microlit Laboratories, Inc. (Madison, NJ).

HPLC hydrolysis assays were performed using 25 nM to 3.0 μM enzyme in 100 μL volumes at 30 °C containing 50 mM HEPES-KOH (pH 7.8), 100 mM NaCl, 20% glycerol, 5 mM DTT, and the appropriate amount of substrate (in DMSO), with or without NS4A peptide, such that the final concentration of DMSO did not exceed 4%. Separate control experiments verified that this percentage of DMSO did not effect enzymatic activity. Cleavage reactions were quenched by the addition of an equal volume of a mixture of 10% TFA/acetonitrile (1/1), and activity was assessed on a reversed phase HPLC column (Rainin C18 Microsorb-MV, 5 μm, 4.6 × 250 mm; 0 to 50% acetonitrile and 0.1% TFA at 3.33%/min) using a Hewlett-Packard 1050 instrument with autoinjection and diode array detection at 210 and 280 nm (where appropriate). Peptide elution fragments were collected and identified by mass spectrometry and N-terminal sequence analysis. Fragment identity and concentration were further verified by authentic, synthesized products. Initial rates of hydrolysis were determined at <20% substrate conversion, and catalytic parameters were determined by fitting rate *vs* [substrate] data to the Michaelis−Menten equation using MultiFit (Day Computing, Cambridge, MA).

Spectrophotometric assays were run in a 96-well microtiter plate at 30 °C, using a SpectraMax 250 reader (Molecular Devices, Sunnyvale, CA) with kinetic capability. Cleavage of EDVVαAbuC-*p*-nitroanilide (5A-*p*NA) substrate was performed with or without NS4A in the identical buffer used for HPLC assays at 30 °C, and pNA release was monitored at 405 nm. The extinction coefficient of *p*-nitroaniline is independent of pH at values of 5.5 and above (Tuppy et al., 1962; S. A. Raybuck and Y. P. C. Luong, unpublished observations). The percentage of DMSO did not exceed 4% in these assays.

Determination of the pH dependence of V_{max}/K_m was performed using a series of constant ionic strength buffers containing 50 mM MES, 25 mM Tris, 25 mM ethanolamine, and 0.1 M NaCl in the pH range of 5.5−9.5 (Morrison & Stone, 1988). The inflection points for log(V/K) data were calculated by nonlinear least-squares fit of the data to the following equation (Dixon & Webb, 1979)

$$\log v = \log[V_{max}/(1+H/K_a + K_b/H)]$$

using the program KineTic (BioKin Ltd.).

Kinetic constants for the rapid equilibrium-ordered bisubstrate reactions were determined from rate *vs* [4A], [EDVVαAbuC-pNA], and [EDVVαAbuCSMSY] data by nonlinear least-squares fitting to eq 1 (Morrison, 1969) as described in the text. K_{ii} and K_{is} values for peptidyl inhibitors were determined from rate *vs* [inhibitor] and [substrate] data and fitting to the equation for mixed inhibition:

$$\text{rate} = V_{max}[S]/[K_m(1 + [I]/K_{is}) + [S](1 + [I]/K_{ii})]$$

The commercial program KinetAsyst II (IntelliKinetics, State College, PA) was used for both procedures. K_i values were calculated from rate *vs* [inhibitor] plots by a nonlinear least-squares fit of the data to the equation of Morrison for tight binding competitive inhibition (Morrison, 1969). The KineTic program (BioKin Ltd.) was used for this procedure.

Table 1: Effect of the NS4A Peptide on the Hydrolysis Kinetics of HCV Synthetic Peptide Substrates[a]

substrate	k_{cat} with or without 4A (s^{-1})	K_m with or without 4A (μM)	k_{cat}/K_m with or without 4A ($M^{-1}\,s^{-1}$)
5A/5B	0.6 ± 0.007	32 ± 2	20000
	0.18 ± 0.01	270 ± 38	700
4A/4B	0.26 ± 0.005	160 ± 11	1600
	0.05 ± 0.0002	805 ± 73	60
4B/5A	ND	ND	110
	ND	ND	4
5A-pNA	0.2 ± 0.005	1010 ± 157	200
	0.012 ± 0.002	1080 ± 167	10

[a] Hydrolysis reactions were performed as described in Experimental Procedures in the presence of 30 μM KK4A1678−1691. Peptide sequences are as follows: 5A/5B, EDVVαAbuC*SMSY; 4A/4B, DEMEEC*SQHLPYI; 4B/5A, ECTTPC*SGSWLRD; and 5A-pNA, EDVVαAbuC*-pNA. The asterisks indicate the site of hydrolysis.

Substrate Model. The substrate [sequence] was modeled in the NS3 protease on the basis of available data for ligands bound to chymotrypsin fold proteins available in the Protein Data Bank. The procedure used was essentially that as described by Love et al. (1996). Figure 4 was generated with GRASP (Nicholls et al., 1991).

RESULTS

Activity of Synthetic Peptide Substrates. The catalytic specificity of purified protease toward various polyprotein hydrolytic sites, re-created in small substrate peptides, was addressed in the absence and presence of NS4A. As shown in Table 1, the observed rate of hydrolysis of peptidyl substrates is sequence-site-dependent. The peptide encompassing the NS5A/NS5B cleavage site was hydrolyzed most efficiently. This peptide was chosen as the parent substrate for a number of studies (*vide infra*). Substitution of α-aminobutyric acid for Cys, the naturally occurring P_2 residue in this substrate cleavage site, had no effect on catalytic parameters and let us avoid potential problems arising from the adjacent Cys residue (data not shown). Although the 5A/5B cleavage sequence is more hydrophobic than the 4A/4B cleavage sequence, solubility problems were not encountered. The peptide encompassing the NS4B/NS5A cleavage site was hydrolyzed least efficiently. The NS3/NS4A cleavage site was excluded from our substrate peptide studies, as it is a *cis* cleavage site. In all cases, proteolytic activity was significantly increased in the presence of an NS4A peptide. The NS4A peptide used in this study re-creates amino acids 1678−1691 of the virus polyprotein sequence with a Cys → Ser substitution at position 1679 and contains two N-terminal lysine residues introduced to increase solubility (Kim et al., 1996). The resulting amino acid sequence is H-KKGSVVIVGRIVLSGK-OH. This NS4A peptide is designated KK4A and contains the hydrophobic core of the 54-residue NS4A protein shown to be essential for enhanced protease activity (Lin et al., 1995; Bukiewicz et al., 1996). Control experiments were conducted in the absence of tNS3 protease to verify that KK4A does not contain an endogenous hydrolytic activity on peptide substrates (data not shown). The presence of KK4A increased k_{cat} and decreased K_m of tNS3 protease for HPLC substrates NS5A/NS5B and NS4A/4B (Table 1). KK4A peptide increased k_{cat} for the spectrophotometric substrate 5A-pNA. In addition, as measured by k_{cat}/K_m, the specificity

toward HPLC substrate 4B/5A was dramatically improved in the presence of KK4A.

In order to determine whether the increased rate of hydrolysis of peptide substrates in the presence of KK4A was due to a perturbation of active site pK_a values, the pH dependence of tNS3-catalyzed processing of 5A/5B-derived substrates EDVVαAbuC-pNA and EDVVαAbuCSMSY was investigated as described in Experimental Procedures. The pH dependence of *V*/*K* for the chromophoric substrate EDVVαAbuC-pNA catalyzed by tNS3 protease alone exhibits a narrow bell-shaped curve which can be fit to pK_a values of 7.2 and 8.5 for the acidic and basic limbs, respectively (data not shown). In the presence of KK4A, an increase in the rate of hydrolysis is observed which is typical of the activating effect of KK4A. However, the profile of the curve is unchanged, and a fit of the data yields identical values of 7.2 and 8.5. A similar determination of the pH dependence of hydrolysis of the decapeptide substrate EDVVαAbuCSMSY under *V*/*K* conditions gave pK_a values of 7.2 and 8.5, indicating that the profile is independent of the choice of peptide substrate. The virtually identical profiles indicate that the pH dependence of protease hydrolysis reactions is NS4A-independent.

Role of NS4A in Catalysis. The stimulatory effect of NS4A on tNS3 protease-catalyzed cleavage of synthetic peptide substrates merited further investigation. The *p*-nitroanilide substrate EDVVαAbuC-pNA (5A-pNA) was employed as a convenient spectrophotometric probe of protease activity.

In the absence of the KK4A peptide, the 5A-pNA substrate is turned over slowly by the protease; $k_{cat} = 0.012 \pm 0.002$ s^{-1}, $K_m = 1000 \pm 200$ μM. In the presence of 30 μM KK4A, a significant increase in protease activity is seen which is due entirely to an increase in k_{cat} to 0.20 ± 0.01 s^{-1}; K_m remains constant at 1100 ± 200 μM (Table 1). Given that KK4A increases protease activity by more than 1 order of magnitude, this peptide can be considered an essential activator. We began this study by exploring the mechanism of this activation.

In a kinetic experiment designed to study bisubstrate reactions, initial velocities of 5A-pNA cleavage were measured at varying concentrations of both KK4A and 5A-pNA, keeping the concentration of the protease fixed. The corresponding reciprocal plots are shown in Figure 2. Figure 2A shows the inverse velocities plotted against inverse KK4A concentration and gives a pattern of straight lines intersecting in the first quadrant to the left of the vertical axis. When these same inverse velocities are plotted *vs* the inverse 5A-pNA concentrations (Figure 2B), the pattern of lines now intersects directly on the vertical axis, not to the left. The intercept replot of the individual lines *vs* 1/[KK4A] is constant, and the slope replot *vs* 1/[5A/5B] from Figure 2A passes through the origin (data not shown). This replot pattern is diagnostic of an equilibrium-ordered kinetic mechanism in which the addition of the activator occurs under equilibrium conditions and must precede the binding of the 5A-pNA substrate. As an activator, KK4A need not dissociate during each catalytic cycle; however, it must not dissociate once the *p*-nitroanilide substrate is bound (Cleland, 1970). Likewise, prior binding of the 5A-pNA substrate to the protease (which must occur as shown by the turnover in the absence of KK4A) prevents subsequent binding and activation by KK4A. Nonlinear least-squares fitting of the

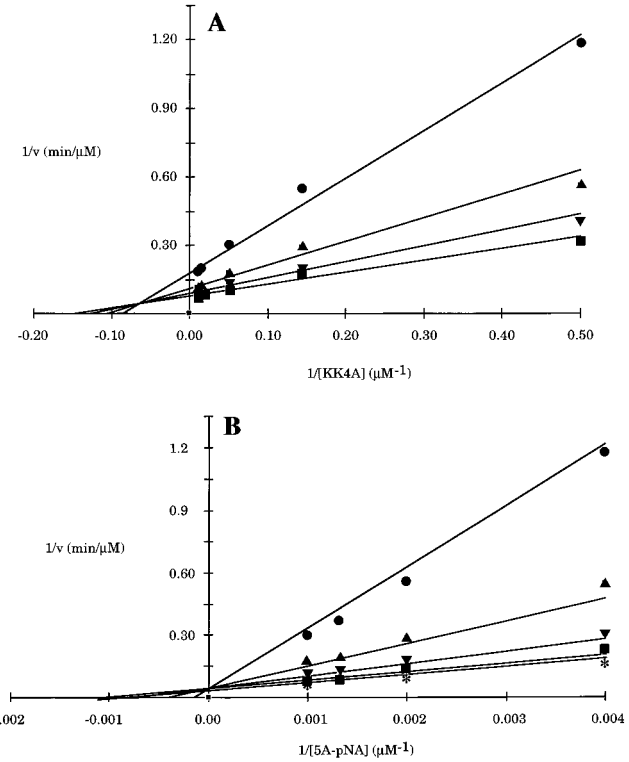

FIGURE 2: (A) 1/*v vs* 1/[KK4A] plot in the presence of fixed levels of 5A-pNA. The concentrations of 5A−pNA are 0.25 (●), 0.5 (▲), 0.75 (▼), and 1.0 (■) mM; the concentrations of KK4A are 2, 7, 20, 70, and 100 μM. The lines indicate a nonlinear least-squares fit of the data to a rapid equilibrium-ordered bireactant model where KK4A binds before 5A−pNA. (B) 1/*v vs* 1/[5A−pNA] plot of the same data set in the presence of fixed levels of KK4A [2 (●), 7 (▲), 20 (▼), 70 (■), and 100 (*) μM]. The lines indicate a nonlinear least-squares fit of the data to the same model as in panel A. See Experimental Procedures for details.

complete data set to eq 1 for an equilibrium-ordered bisubstrate reaction gives the following kinetic parameters: $k_{cat} = 0.20 \pm 0.02$ s^{-1}, $K_{ia} = 22 \pm 3$ μM, and $K_b = 660 \pm 130$ μM.

$$v = \frac{k_{cat}[E]_t[A][B]}{K_{ia}K_b + K_b[A] + [A][B]} \quad (1)$$

We have confirmed that this kinetic scheme is not unique to the chromophoric substrate. Analysis of the data for hydrolysis of the decapeptide EDVVαAbuCSMSY gives a similar equilibrium-ordered pattern with the following kinetic parameters: $k_{cat} = 0.53 \pm 0.04$ s^{-1}, $K_{ia} = 20.0 \pm 3.5$ μM, and $K_b = 18 \pm 3.0$ μM (data not shown).

An active site inhibitor was then employed to confirm the kinetic model. EDVVαAbuCPαAbuSY-OH is a variant of the 5A cleavage site. Introduction of Pro into the P_1' position of this peptide results in a peptide that is not hydrolyzed as a substrate (*vide infra*) but inhibits the enzyme in the presence of efficiently processed substrates. This compound shows an inhibition pattern which is competitive with respect to the substrate 5A-pNA and has a K_i of 80 ± 7.0 μM under standard conditions of [KK4A] = 30 μM (data not shown). If the ordered model for 4A activation is correct and the peptide binds only to the fully activated protease, an uncompetitive inhibition pattern is expected when the decapeptide inhibitor is assayed *vs* various fixed concentrations of the KK4A activator. The reciprocal plot representing the data from this experiment is shown in Figure 3A, and reveals

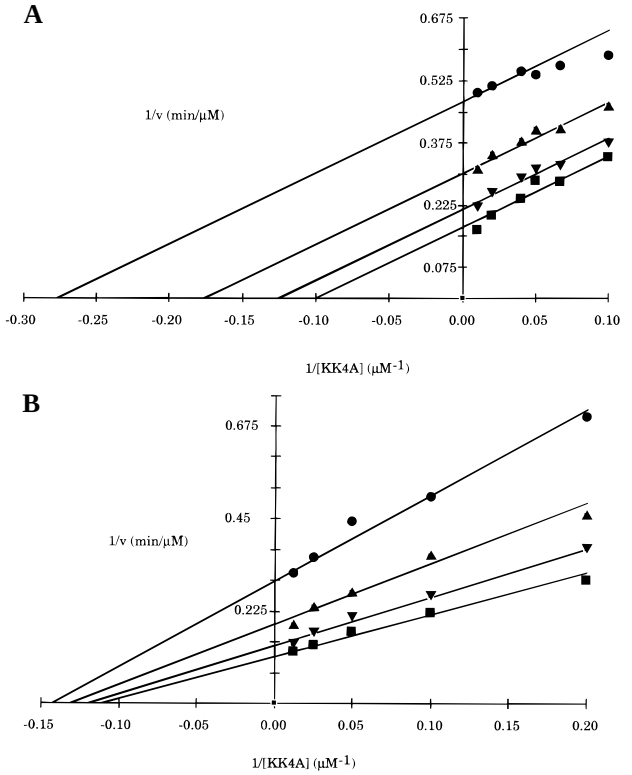

FIGURE 3: (A) $1/v$ *vs* 1/[KK4A] plot in the presence of fixed levels of decapeptide inhibitor EDVVαAbuCPαAbuSY and constant 5A−pNA (0.5 mM). The concentrations of inhibitor are 200 (●), 100 (▲), 50 (▼), and 25 (■) μM; the concentrations of KK4A are 1.5, 2.5, 5.0, 10.0, 15.0, 20.0, 25.0, 50.0, and 100 μM. The lines indicate a nonlinear least-squares fit of the data to an uncompetitive model where KK4A binding must precede EDVVαAbuCPαAbuSY binding. (B) $1/v$ *vs* 1/[KK4A] plot in the presence of fixed levels of aldehyde inhibitor EDVVαAbuV-CHO and constant 5A−pNA (1.0 mM). The concentrations of inhibitor are 200 (●), 100 (▲), 50 (▼), and 25 (■) μM; the concentrations of KK4A are 5.0, 10.0, 20.0, 40.0, 80.0, and 100.0 μM. The lines indicate a nonlinear least-squares fit of the data to a noncompetitive model where EDVVαAbuV-CHO binding may precede or follow KK4A binding. See Experimental Procedures for details.

a set of parallel lines which are characteristic of uncompetitive inhibition. Nonlinear least-squares fitting of the data rules out a mixed inhibition pattern; any contribution to the inhibition from the slope term (K_{is}) is very much greater than the measured K_{ii} value of 75 ± 6 μM. The K_{is} term reflects the binding of inhibitor to the free, unactivated protease and is competitive with KK4A. The value of this term can be independently determined by assaying the inhibitor against the unactivated protease in the absence of KK4A. A K_i of 2.3 mM was measured for inhibition of the free enzyme under these conditions, a value which is 30-fold higher than the affinity of the inhibitor for the activated protease and confirms the uncompetitive inhibition pattern observed above.

With the equilibrium-ordered kinetic mechanism confirmed, we next sought to use additional inhibitors to delineate the role of NS4A in modifying the active site of the protease. An aldehyde inhibitor, EDVVαAbuV-CHO, was chosen as it lacks any of the prime-side residues. The double-reciprocal plot for inhibition of protease activity at varying KK4A concentrations is shown in Figure 3B. In this case, the pattern observed is one of intersecting and not parallel lines, indicative of mixed inhibition and suggesting that appreciable binding of the aldehyde inhibitor to the protease occurs both in the presence and in the absence of KK4A. The measured inhibition constants of 50 ± 5.0 μM (with 4A) and 65 ± 5.0 μM (without 4A) are in good agreement with the above results. The above data are consistent with the notion of two distinct classes of inhibitors: an NS4A-dependent class which binds to protease subsequent to NS4A binding and an NS4A-independent class whose binding to protease is not affected by the presence of 4A.

Table 2: Catalytic Consequences of P_1 Substitutions on 5A/5B Substrate Hydrolysis[a]

P_1 residue	k_{cat} (s^{-1})	K_m (μM)	k_{cat}/K_m (M^{-1} s^{-1})	K_i (μM)
Cys	0.61 ± 0.2	32 ± 2	20000	–
Abu	0.06 ± 0.003	110 ± 18	580	–
SMeCys[b]	0.049 ± 0.003	130 ± 20	385	–
Thr	0.024 ± 0.002	145 ± 25	165	–
Ala	0.022 ± 0.005	815 ± 205	25	–
Val	0.005 ± 0.0004	550 ± 67	9	–
Leu	–	–	5	–
Tyr	–	–	–	>700
Asp	–	–	–	>700
hPhe[c]	–	–	–	>700
2Nal[d]	–	–	–	>700

[a] Hydrolysis reactions were performed as described in Experimental Procedures in the presence of 30 μM KK4A1678−1691. In all cases, the P_2 and $P_{2'}$ residues were α-aminobutyric acid. [b] Represents *S*-methylcysteine. [c] Represents homophenylalanine. [d] Represents 2-naphthylalanine.

Structure−Activity Relationship at P_1 and P_1' of 5A/5B. In order to probe the substrate specificity of tNS3 protease, a number of natural and non-natural amino acid substitutions were introduced at the P_1 and P_1' positions of the 5A/5B substrate EDVVαAbuCSαAbuSY and tested using the HPLC hydrolysis assay in the presence of KK4A peptide. In this peptide series, α-aminobutyric acid replaces Met in the P_2' position. This substitution was shown to be without catalytic consequence (data not shown). The protease exhibits a marked preference toward cysteine at P_1, the residue most commonly found at this position in naturally occurring substrates (Table 2). Methylation of cysteine sulfhydryl or substitution by the ethyl side chain has a dramatic but tolerable effect on activity, decreasing k_{cat} by 1 order of magnitude and increasing K_m. As indicated by the P_1 Ala substrate, specificity is dependent upon enzyme−substrate interactions beyond an α side chain methylene group. However, as shown by the decrease in k_{cat}/K_m exhibited by P_1 Leu and Val substitutions, α-branching has deleterious catalytic consequences. The absence of binding of P_1 Asp indicates that presumed negative charge at this position is alone not a specificity determinant. The pK_a of Cys at this position is 8.2 and is therefore expected to have some negative charge character under our assay conditions. However, in the case of Asp, negative charge is apparently insufficient to compensate for branching. Finally, natural (Tyr) or non-natural, bulky aromatics (2-naphthylalanine) exhibit a complete lack of binding to the tNS3 protease.

A similar analysis at the P_1' position (Table 3) indicates the protease exhibits a catalytic preference toward serine, the residue frequently found in naturally occurring substrates. As opposed to the trend observed at P_1 (substitutions decrease both k_{cat} and affinity), substitutions at P_1' decreased k_{cat} but had varied effects on affinity. Substrates containing P_1' residues of Ala, Tyr, Phe, or Trp exhibit K_m values within 2-fold of that of Ser. Substitution of a D-amino acid, a

Table 3: Catalytic Consequences of P_1' Substitutions on 5A/5B Substrate Hydrolysis[a]

P_1' residue	k_{cat} (s^{-1})	K_m (μM)	k_{cat}/K_m (M^{-1} s^{-1})	K_i (μM)
Ser	0.61 ± 0.02	32 ± 2	20000	–
2Nal[b]	0.016 ± 0.002	40 ± 9	400	–
Phe	0.012 ± 0.0005	33 ± 5	350	–
Trp	0.008 ± 0.0005	33 ± 8	250	–
Phg[c]	0.01 ± 0.0005	205 ± 32	50	–
Tic[d]	–	–	–	4 ± 0.2
Pip[e]	–	–	–	18 ± 5
D-Ser	–	–	–	>700
Lys[f]	0.09 ± 0.006	2000 ± 210	45	–
Ala	0.1 ± 0.006	70 ± 14	1400	–
Asp	0.09 ± 0.005	205 ± 30	450	–
Tyr	0.013 ± 0.001	70 ± 18	190	–
Pro	–	–	–	80 ± 1

[a] Hydrolysis reactions were performed as described in Experimental Procedures in the presence of 30 μM KK4A1678−1691. [b] Represents 2-naphthylalanine. [c] Represents phenylglycine. [d] Represents tetrahydroisoquinoline-3-carboxylic acid. [e] Represents pipecolinic acid. [f] This reaction and subsequent hydrolysis reactions were performed in the presence of a NS4A peptide identical to KK4A but lacking terminal lysine residues.

positively charged (Lys) or a negatively charged (Asp) residue, decreased affinity. Substitution of bulky cyclic aromatics (Tic) or smaller cyclic alkyls (Pro or Pip) yielded peptides which were not hydrolyzed under our standard assay conditions ($k_{cat}/K_m < 0.5$ M^{-1} s^{-1}). However, this latter class of peptides maintain a high affinity for the protease as indicated by the observed K_i values (Table 3). These noncleavable substrate analogues were highly useful as probes of mechanism and pocket selectivity.

Effect of KK4A on the Binding of Peptidyl Inhibitors to tNS3 Protease. The modulatory effect that KK4A imparts on the active site of tNS3 protease was investigated. The potency of peptide inhibitors truncated from the prime (**2**−**4**) and P (**5**−**8**) sides was measured in the absence and presence of KK4A (Table 4). The decapeptide inhibitor containing the P_1' residue tetrahydroisoquinoline-3-carboxylic acid (Tic) having the sequence E-D-V-V-L-C-Tic-Nle-S-Y was used as the parental peptide (**1**) for both series. P_2 Leu and P_2' Nle residues increased the affinity of the inhibitor for protease.

A comparison of K_i values of inhibitors from each series determined for the tNS3−NS4A complex is presented in the third column of Table 4. Deletion of up to three prime residues, P_4'−P_2' of the decapeptide (**1** *vs* **4**), results in a 40-fold increase in K_i, from 0.34 to 14 μM. However, stepwise truncation of residues from the P side results in a dramatically decreased affinity of the peptide inhibitor for tNS3−NS4A. The value of K_i increases from 0.34 to 2000 μM, nearly 6000-fold, with the deletion of four P residues (**1** *vs* **8**). Therefore, most of the binding energy of this decapeptide is due to interactions with the tNS3−NS4A complex on the P side of the inhibitor.

Inspection of the K_i values determined for inhibitors from each series in the presence (column 3, Table 4) and absence of NS4A (column 4, Table 4) reveals the region of the peptide inhibitor where interactions with tNS3 are most influenced by NS4A. The 40-fold difference in K_i values between **4** and **1** determined for the tNS3−NS4A complex (14 *vs* 0.34 μM, column 3) is reduced to a 4.3-fold difference for tNS3 protease alone (120 *vs* 28 μM, column 4). However, the without NS4A/with NS4A ratio of these K_i values is reduced from a 83-fold difference (28 *vs* 0.34 μM) for inhibitor **1** to an 8.4-fold difference (120 *vs* 14 μM) for inhibitor **4**. Comparison of the K_i values determined for **6** *vs* **1** in the presence of NS4A (column 3, 79 *vs* 0.34 μM; 230-fold) and in the absence of NS4A (column 4, 2700 *vs* 28 μM; 100-fold) indicates the without NS4A/with NS4A K_i ratio is reduced a mere 2.3-fold. When the same comparison is made for **5** *vs* **1**, the without NS4A/with NS4A K_i ratio is reduced 1.1-fold. This analysis suggests that the greatest effect of NS4A can be found in interactions on the prime side of these inhibitors. The large increase in K_i values in the absence of KK4A with peptidyl inhibitors which contain the full array of prime-side residues renders determination of the K_i value for **7** difficult; no inhibition could be detected at 1 mM peptide inhibitor, and only a lower limit of 13 mM could be estimated.

The prime-side subsites of tNS3 protease influenced most dramatically by NS4A can be assigned by comparing the value of K_i determined for inhibitors **1**−**4** in the presence and absence of NS4A. The without NS4A/with NS4A K_i ratio exhibits a significant decrease upon deletion of P_4' (**1** *vs* **2**, 83 *vs* 15), demonstrating a substantial interaction between KK4A and the S_4' subsite, which is occupied by tyrosine in the 5A/5B series. The without NS4A/with NS4A ratio remains constant as P_3' and P_2' are truncated (**1** *vs* **3** and **4**, 83 *vs* 9.0 and 8.0, respectively), suggesting that NS4A makes no significant contribution to the binding of residues at these positions. Alternatively, the residues Nle and Ser at the P_2' and P_3' positions, respectively, may not be optimized to detect contributions in these peptides. In contrast, the modulatory effect of the KK4A peptide is markedly dependent upon the presence of a P_1' residue. Peptide **4** which contains a P_1' residue maintains a without NS4A/with NS4A ratio of 8.0, demonstrating a 1 order-of-magnitude greater potency in the presence of KK4A. Truncation beyond P_1' renders peptides which inhibit tNS3 protease *via* an NS4A-independent mechanism. This phenomenon is most apparent by comparing inhibitor **4** (Table 4) to the aldehyde inhibitor EDVVαAbuV-CHO. The K_i values determined for this inhibitor are 50 and 65 μM in the presence and absence of KK4A, respectively. The truncated spectrophotometric substrate 5A-pNA exhibits an increase in k_{cat} of greater than 1 order of magnitude in the presence of NS4A, also supporting a role for 4A near the site of hydrolysis when the S_1' pocket is occupied (albeit by an nonnatural residue in this case). In contrast, deletion of residues from the P side of the inhibitor (**1** *vs* **5** and **6**) has little effect on the without NS4A/with NS4A K_i ratio.

DISCUSSION

Many investigations have focused on the mechanism by which NS3 protease processes downstream gene products, and a number of hypotheses have been proposed to explain the activation of NS3 protease by NS4A cofactor. These include membrane anchoring, enhanced protease stability, alteration of cleavage site specificity and enhanced substrate recognition *via* alterations in subsite pockets (Failla et al., 1994, 1995; Lin et al., 1994b, 1995; Satoh et al., 1995; Steinkuhler et al., 1996a). The present study is the first investigation which utilizes a number of kinetic tools and substrate-derived peptide inhibitors to delineate the mechanistic role of NS4A in the tNS3−NS4A complex.

Table 4: Effect of Prime and Nonprime Truncations on K_i of P_1' Tic Decapeptide Inhibitors

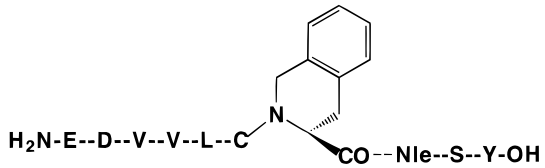

number	sequence	K_i with 4A (μM)	K_i without 4A (μM)	without 4A/with 4A ratio
1	H_2N-E-D-V-V-L-C-Tic-Nle-S-Y-OH	0.34	28	83
2	H_2N-E-D-V-V-L-C-Tic-Nle-S-OH	27	380	14.5
3	H_2N-E-D-V-V-L-C-Tic-Nle-OH	17	140	8.6
4	H_2N-E-D-V-V-L-C-Tic-OH	14	120	8.4
5	H_2N-D-V-V-L-C-Tic-Nle-S-Y-OH	4.4	320	73
6	H_2N-V-V-L-C-Tic-Nle-S-Y-OH	79	2700	34
7	H_2N-V-L-C-Tic-Nle-S-Y-OH	500	NI at 1 mM[a]	>26
8	H_2N-L-C-Tic-Nle-S-Y-OH	2000	NI at 1 mM	

[a] In the absence of an inhibition of 5% that would have been detected by our assay system, a lower limit of 13 mM can be set for the K_i of this peptide in the absence of KK4A.

For all substrates investigated, hydrolysis rates were enhanced in the presence of the NS4A peptide. The k_{cat}/K_m values measured for the various peptide substrates are increased 20−30-fold (Table 1). The magnitude of this stimulatory effect is similar to that observed by Shimizu et al. using an *in vitro* system composed of a synthetic NS4A peptide containing residues 18−40 of NS4A and recombinantly expressed full length NS3 (Shimizu et al., 1996). Therefore, the large rate enhancements seen in the presence of KK4A for tNS3 protease-catalyzed hydrolysis of peptides based upon downstream processing sites are specific to the protease domain and are maintained upon deletion of the helicase domain from the C terminus of the full length NS3 protein.

One potential explanation for the observed stimulatory effect provided by NS4A is that it orchestrates a favorable alignment of titratable catalytic groups within the active site. While rarely straightforward, the interpretation of pH effects on catalytic groups is exacerbated by the complexity of this system. The similar pK_a values extracted from the *V*/*K* *vs* pH data for the extended decapeptide substrate and the truncated chromophoric substrate indicate that the $P_4'-P_2'$ residues do not contribute to the observed pH rate profile. Given the numerous ionizations in the P region of substrate (N-terminal amine, neighboring Glu and Asp residues, and Cys), it is likely that substrate contributes to the observed pH rate profile, and this complicates the dissection and assignment of pK_a values to individual protease residues. However, our observation that KK4A does not alter log *V*/*K* *vs* pH profiles strongly suggests that KK4A does not increase catalytic activity of the protease by a perturbation of the pK_a values for the active site residues involved in catalysis.

The specific interactions which are observed in the tNS3−NS4A complex result in a substantial increase in catalytic efficiency and are further reflected in the obligate order kinetic mechanism proposed here. After hydrolysis of substrate, product is released from the protease−4A complex (Scheme 1, pNA release and 5A−acyl-enzyme hydrolysis/release are indicated as a single step). The proposed mechanism may reflect the catalytic cycle within HCV-infected cells and is validated by the three-dimensional structure of the co-complex. While a faithful *in vivo* replication system is not currently available, it is likely, on the basis of the above evidence, that NS3−NS4A complex

Scheme 1: Kinetic Model Depicting the Role of NS4A in Substrate Hydrolysis and Inhibitor Binding[a]

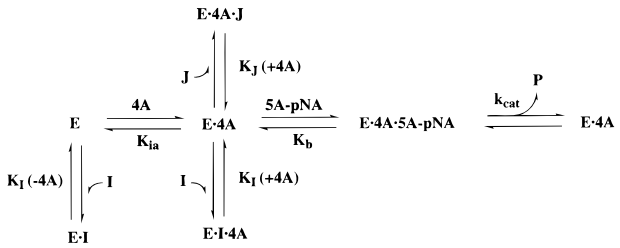

[a] **J** represents an inhibitor having prime-side residues. **I** represents an inhibitor lacking prime-side residues.

formation precedes hydrolysis of downstream sites and that the complex remains associated between catalytic events.

The P_1 substitution data presented in Table 2, demonstrating a catalytic preference for Cys, are supported by modeling and mutagenesis studies (Pizzi et al., 1994; Failla et al., 1996) as well as structural information (Kim et al., 1996; Love et al., 1996). Structural information indicates a shallow S_1 pocket which can accommodate small aliphatic residues. Phe1180 is situated at the bottom of this pocket where favorable van der Waals contacts to the P_1 Cys residue are likely (Kim et al., 1996; Love et al., 1996). This type of interaction is documented (Burley & Petsko, 1988). Modeling studies predicted the location of Phe1180 (Pizzi et al., 1994), and mutagenesis studies verified this substrate recognition mechanism by demonstrating that the double mutant Phe1180Thr/Ala1183Gly, having a larger S_1 specificity pocket, tolerated a bulky Phe residue at P_1 (Failla et al., 1996).

In contrast to the P_1 substitution data, the P_1' substitution data presented in Table 3 indicate that a reduction in the rate of peptide substrate hydrolysis may be accompanied by a reduced or an increased affinity of the peptide for protease. The observation that the decapeptide containing the P_1' Tic residue is a potent inhibitor of the tNS3 protease suggests a relatively open binding pocket. Although less structural information is available concerning the S′ specificity pocket, our data, as well as that of Love et al. (1996), indicate that the S_1' pocket is not fully occupied by P_1' Ser of the modeled substrate, suggesting the potential to accommodate larger residues. While the potent binding of the P_1' Tic decapeptide inhibitor may be a consequence of an altered mode of peptide

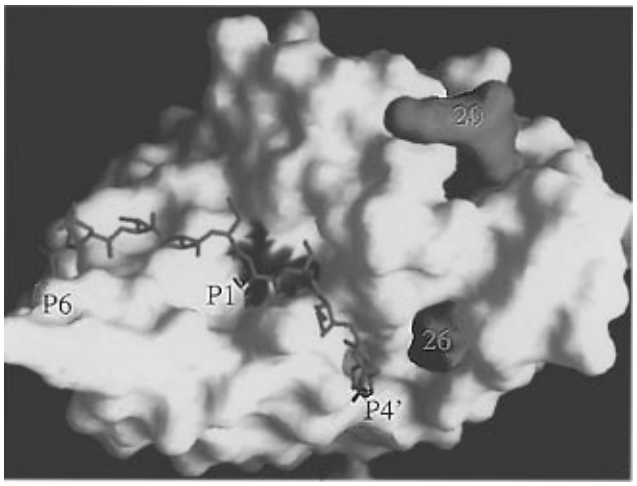

FIGURE 4: Surface representation of the X-ray structure of the truncated tNS3−NS4A co-complex (Kim et al., 1996) with a P_6−$P_{4'}$ decapeptide modeled into the active site. The tNS3 protease surface is white, the NS4A peptide red, and the substrate model green, with the P_1 cysteine sulfhydryl indicated in yellow. The blue batch on the tNS3 surface shows the catalytic serine residue. Residue 1 of the NS4A peptide corresponds to residue 1678 in the polyprotein sequence. The figure was generated with GRASP (Nicholls et al., 1991).

binding, it is of interest for inhibitor design and provides a basis for probing the effect of NS4A on P′ residues.

The K_i data for the petidyl P_1' Tic series presented in Table 4 reveal three critical features of the interaction of peptidyl inhibitors with the tNS3 protease. First, most of the binding energy for a given inhibitor is extracted from the P side by tNS3 protease. This observation is true irrespective of KK4A and is consistent with observations made with other serine (Powers & Harper, 1986) as well as cysteine proteases (Rich, 1986). Second, in all cases, the affinity of inhibitor for protease is increased in the presence of KK4A peptide. Third, the prime-side subsites of tNS3 protease influenced most dramatically by KK4A are S_4' and S_1'. In order to correlate these latter two observations with the available structural data, a decapeptide substrate (sequence) ranging from P_6 to P_4' was modeled into the active site of the tNS3−NS4A complex (Figure 4). From this model, it appears likely that the P_4' substrate Tyr residue is in close proximity to NS4A and may be in direct contact. This is consistent with the large loss in binding of inhibitors which extend to P_4' upon removal of NS4A. In addition, NS4A makes substantial contacts with several loops on the prime side of the subtrate binding channel. Removal of NS4A is likely to perturb these loops, which make contact with the P_1'−P_3' residues of substrate. This is consistent with the experimental data, which show a decrease in the magnitude of K_i of 1 order of magnitude upon removal of NS4A. Aldehyde inhibitors do not extend into the prime side and would not be expected to be as dramatically affected by the presence or absence of NS4A. Experimentally, the K_i value measured for aldehyde inhibitors with the tNS3 protease is the same as that for the tNS3−NS4A complex.

The dependency of HCV protease activity on the presence of a virus-encoded peptidyl activator is not unique. Human adenovirus-2 L3 23K protease (AVP) binds an 11-amino acid cofactor encoded by the C terminus of the pVI protein (pVIc; Webster et al., 1993) in a 1/1 stoichiometry which increases k_{cat} of this cysteine protease by 350-fold (Mangel et al., 1996). Structural analysis revealed that the pVIc peptide is surface-bound, distant from the active site (Ding et al., 1996). Activation of AVP by pVIc has been proposed to occur *via* alterations in the active site imparted by interactions of the peptide with noncontiguous segments of protease. In addition to HCV, the two other genera of the Flaviviridae family, the pestiviruses and flaviviruses, also rely upon a two-component protease. The genetic organization and the processing of the bovine viral diarrhea virus (BVDV; a member of the *Pestivirus* genus) polyprotein is analogous to that of HCV. Wiskerchen and Collet (1991) have shown that p80, the BVDV NS3 homologue, requires p10. This small virally encoded peptide is released from the polyprotein and is required for efficient hydrolysis of p58-p75, the BVDV NS5A/5B homologue. As discussed by Fallia et al. (1994), p10 is likely an NS4A functional homologue. Within the *Flavivirus* genus, the absolute requirement of a virus-encoded activator for efficient polyprotein processing at structural and nonstructural sites has also been demonstrated (Wengler et al., 1991; Chambers et al., 1993; Falgout et al., 1993). A 40-amino acid consensus peptide within the NS2B domain of flaviviruses has been shown to be required for *trans* complementation of NS3 proteolytic activity in yellow fever (Chambers et al., 1993) and dengue viruses (Falgout et al., 1993). NS2B, which occurs N-terminal to NS3, is analogous to HCV NS4A in that it may function in *cis* or in *trans* and it is released from its catalytic domain *via* an intramolecular cleavage. The mechanism of action of the NS4A activator elucidated here for HCV tNS3−NS4A may well be a general phenomenon within the *Flaviviridae* family.

ACKNOWLEDGMENT

We thank Stephen Chambers, John Fulghum, and Robert McCarrick for fermentations; Joyce Coll and Maureen Dwyer for protein purification; Mark Fleming for protein sequencing and microanalysis; Paul Caron and Mark Murcko for helpful discussions and contributions to Figure 4; and William Markland, John Thomson, and Vicki Sato for a critical reading of the manuscript.

REFERENCES

Bartenschlager, R., Ahlborn-Laake, L., Mous, J., & Jacobsen, H. (1993) *J. Virol. 67*, 3835−3844.

Bukiewicz, N. J., Wendel, M., Zhang, R., Jubin, R., Pichardo, J., Smith, E. B., Hart, A. M., Ingram, R., Durkin, J., Mui, P. W., Murray, M. G., Ramanathan, L., & Dasmahapatra, B. (1996) *Virology 225*, 328−338.

Burley, S. K., & Petsko, G. A. (1988) *Adv. Protein Chem. 39*, 125−189.

Chambers, T. J., Nestorowicz, S. M., Amberg, S. M., & Rice, C. M. (1993) *J. Virol. 67*, 6797−6807.

Choo, Q., Richman, K. H., Ham, J. H., Berger, K., Lee, C., Dong, C., Gallegos, C., Coit, D., Medina-Selby, A., Barr, P. J., Weiner, A. J., Bradley, D. W., Kuo, G., & Houghton, M. (1991) *Proc. Natl. Acad. Sci. U.S.A. 88*, 2451−2455.

Cleland, W. W. (1970) in *The Enzymes* (Boyer, P. D., Ed.) Vol. 2, p 1, Academic Press.

Ding, J., McGrath, W. J., Sweet, R. M., & Mangel, W. F. (1996) *EMBO J. 15*, 1778−1783.

Dixon, M., & Webb, E. C. (1979) *Enzymes*, pp 138−164, Academic Press, New York.

Eckart, M. R., Selby, M., Masiarz, F., Lee, C., Berger, K., Crawford, K., Kuo, C., Kuo, G., Houghton, M., & Choo, Q. (1993) *Biochem. Biophys. Res. Commun. 192*, 399−406.

Failla, C., Tomei, L., & De Francesco, R. (1994) *J. Virol. 68*, 3753−3760.

Failla, C., Tomei, L., & De Francesco, R. (1995) *J. Virol. 69*, 1769−1777.
Failla, C. M., Pizzi, E., De Francesco, R., & Tramontano, A. (1996) *Folding Des. 1*, 35−42.
Falgout, B., Miller, R. H., & Lai, C. (1993) *J. Virol. 67*, 2034−2042.
Grakoui, A., McCourt, D. W., Wychowski, C., Feinstone, S. M., & Rice, C. M. (1993a) *J. Virol. 67*, 2832−2843.
Grakoui, A., McCourt, D. W., Wychowski, C., Feinstone, S. M., & Rice, C. M. (1993b) *Proc. Natl. Acad. Sci. U.S.A. 90*, 10583−10587.
Grakoui, A., Wychowski, C., Lin, C., Feinstone, S. M., & Rice, C. M. (1993c) *J. Virol. 67*, 1385−1395.
Hijikata, M., Kato, N., Ootsuyama, M., Nakagawa, M., & Shimotohno, K. (1991) *Proc. Natl. Acad. Sci. U.S.A. 88*, 5547−5551.
Hijikata, M., Mizushima, H., Akagi, T., Mori, S., Kakiuchi, N., Kato, N., Tanaka, T., Kimura, K., & Shimotohno, K. (1993) *J. Virol. 67*, 4665−4675.
Houghton, M. (1996) *Hepatits C viruses*, 3rd ed., pp 1035−1058, Lippincott-Raven, Philadelphia.
Houghton, M., Weiner, A., Han, J., Kuo, G., & Choo, Q.-L. (1991) *Hepatology 14*, 381−388.
Kato, M., Hijikata, M., Ootsuyama, Y., Nakagawa, M., Ohkoshi, S., Sugimura, T., & Shimotohno, K. (1990) *Proc. Natl. Acad. Sci. U.S.A. 87*, 9524−9528.
Kim, J. L., Morgenstern, K. A., Lin, C., Fox, T., Dwyer, M. D., Landro, J. A., Chambers, S. P., Markland, W., Lepre, C. A., O'Malley, E. T., Harbeson, S. L., Rice, C. M., Murcko, M. A., Caron, P. R., & Thomson, J. A. (1996) *Cell 87*, 343−355.
Kuo, G., Choo, Q.-L., Alter, H. J., Gitnick, G. L., Redecker, A. G., Purcell, R. H., Myamura, T., Dienstag, J. L., Alter, M. J., Syevens, C. E., Tagtmeyer, G. E., Bonino, F., Colombo, M., Lee, W. S., Kuo, C., Berger, K., Shister, J. R., Overby, L. R., Bradley, D. W., & Houghton, M. (1989) *Science 244*, 362−364.
Lin, C., Lindenbach, B. D., Pragai, B., McCourt, D. W., & Rice, C. M. (1994a) *J. Virol. 68*, 5063−5073.
Lin, C., Pragai, B. M., Grakoui, A., & Rice, C. M. (1994b) *J. Virol. 68*, 8147−8157.
Lin, C., Thomson, J. A., & Rice, C. M. (1995) *J. Virol. 69*, 4373−4380.
Love, R. A., Parge, H. E., Wickersham, J. A., Hostomsky, Z., Habuka, N., Moomaw, E. W., Adachi, T., & Hostomska, Z. (1996) *Cell 87*, 331−342.
Manabe, S., Fuke, I., Tanishita, O., Kaji, C., Gomi, Y., Yoshida, S., Mori, C., Takamizawa, A., Yoshida, I., & Okayama, H. (1994) *Virology 198*, 636−644.
Mangel, W. F., Toledo, D. L., Brown, M. T., Martin, J. H., & McGrath, W. J. (1996) *J. Biol. Chem. 271*, 536−543.
Miller, R. H., & Purcell, R. H. (1990) *Proc. Natl. Acad. Sci. U.S.A. 87*, 2057−2061.
Mizushima, H., Hijikata, M., Tanji, Y., Kimura, K., & Shimotohno, K. (1994) *J. Virol. 68*, 2731−2734.
Morrison, J. F. (1969) *Biochim. Biophys. Acta 185*, 269−286.
Morrison, J. F., & Stone, R. F. (1988) *Biochemistry 27*, 5499−5506.
Nicholls, A., Sharp, K. A., & Honig, B. (1991) *Proteins 11*, 281−295.
Pizzi, E., Tramontano, A., Tomei, L., LaMonica, N., Failla, C., Sardana, M., Wood, T., & De Francesco, R. (1994) *Proc. Natl. Acad. Sci. U.S.A. 91*, 888−892.
Powers, J. C., & Harper, J. W. (1986) in *Proteinase Inhibitors* (Barrett, A. J., & Salvesen, G., Eds.) Vol. 12, pp 57−60, Elsevier, Amsterdam.
Rich, D. H. (1986) in *Proteinase Inhibitors* (Barrett, A. J., & Salvesen, G., Eds.) Vol. 12, pp 155−156, Elsevier, Amsterdam.
Satoh, S., Tanji, Y., Hijikata, M., Kimura, K., & Shimotohno, K. (1995) *J. Virol. 69*, 4255−4260.
Schechter, I. B. A. (1967) *Biochem. Biophys. Res. Commun. 27*, 157−162.
Shimizu, Y., Yamaji, K., Masuho, Y., Yokota, T., Inoue, H., Sudo, K., Satoh, S., & Shimotohno, K. (1996) *J. Virol. 70*, 127−132.
Steinkuhler, C., Tomei, L., & De Francesco, R. (1996a) *J. Biol. Chem. 271*, 6367−6373.
Steinkuhler, C., Urbani, A., Tomei, L., Biasiol, G., Sardana, M., Bianchi, E., Pessi, A., & DeFrancesco, R. (1996b) *J. Virol. 70*, 6694−6700.
Takamizawa, A., Mori, C., Fuke, I., Manabe, S., Murakami, S., Fujita, J., Onishi, E., Andoh, T., Yoshida, I., & Okayama, H. (1991) *J. Virol. 65*, 1105−1113.
Tomei, L., Failla, C., Santolini, E., De Francesco, R., & La Monica, N. (1993) *J. Virol. 67*, 4017−4026.
Tuppy, H., Weisbauer, U., & Wintersberger, E. (1962) *Hoppe-Seyler's Z. Physiol. Chem. 329*, 278−288.
Webster, A., Hay, R. T., & Kemp, G. (1993) *Cell 72*, 97−104.
Wengler, G., Czaya, G., Farber, P. M., & Hegemann, J. H. (1991) *J. Gen. Virol. 72*, 851−858.
Wiskerchen, M., & Collet, M. S. (1991) *Virology 184*, 341−350.

BI963054N